

1 The diversity and functional capacity of microbes associated with coastal phototrophs

2

3 Khashiff Miranda^{1,2*}, Brooke L. Weigel^{3,4}, Emily C. Fogarty^{5,6}, Iva A. Veseli⁷, Anne E. Giblin⁸,
4 A. Murat Eren^{5,9}, Catherine A. Pfister^{3,10}

5

⁶ * Corresponding author email: khashiff.miranda.1@ulaval.ca

7 ¹ The College, The University of Chicago, Chicago, IL, 60637, USA

⁸ ² Département de biologie, Université Laval, Québec, QC, G1V 0A6, Canada

9 ³ Committee on Evolutionary Biology, The University of Chicago, Chicago, IL, 60637, USA

⁴ Friday Harbor Laboratories, University of Washington, Friday Harbor, WA 98250, USA

11 ⁵ Department of Medicine, The University of Chicago, Chicago, IL 60637, USA

12 ⁶ Committee on Microbiology, The University of Chicago, Chicago, IL 60637, USA

¹³ ⁷ Biophysical Sciences Program, The University of Chicago, Chicago, IL, 60637, USA

¹⁴ ⁸The Ecosystems Center, The Marine Biological Laboratory, Woods Hole, MA, 02543, USA

15 ⁹ Josephine Bay Paul Center, Marine Biological Laboratory, Woods Hole, MA 02543, USA

¹⁰ Department of Ecology & Evolution, The University of Chicago, Chicago, IL, 60637 USA

18

Abstract

19 Coastal marine phototrophs exhibit some of the highest rates of primary productivity in the
20 world. They have been found to host a diverse set of microbes, many of which may impact the
21 biology of their phototroph hosts through metabolisms that are unique to microbial taxa. Here we
22 characterized the metabolic functions of phototroph-associated microbial communities using
23 metagenomes collected from 2 species of kelp (*Laminaria setchellii* and *Nereocystis luetkeana*)

24 and 3 marine angiosperms (*Phyllospadix scouleri*, *P. serrulatus* and *Zostera marina*), including
25 the rhizomes of two surfgrass species (*Phyllospadix* spp.) and the seagrass *Zostera marina*, and
26 the sediments surrounding *P. scouleri* and *Z. marina*. Using metagenomic sequencing, we
27 describe 72 metagenome assembled genomes (MAGs) that potentially benefit from being
28 associated with macrophytes and may contribute to macrophyte fitness through their metabolic
29 gene content. All host-associated metagenomes contained genes for the use of dissolved organic
30 matter from hosts and vitamin (B₁, B₂, B₇, B₁₂) biosynthesis. Additionally, we found a range of
31 nitrogen metabolism genes that transform dissolved inorganic nitrogen into forms that may be
32 more available to the host. The rhizosphere of surfgrass and seagrass contained genes for
33 anaerobic microbial metabolisms, including *nifH* genes associated with nitrogen fixation, despite
34 residing in a well-mixed and oxygenated environment. The range of oxygen environments
35 engineered by macrophytes likely explains the diversity of both oxidizing and reducing microbial
36 metabolisms, and contributes to the functional capabilities of microbes and their influence on
37 carbon and nitrogen cycling in nearshore ecosystems.

38

39

Importance

40 Kelps, seagrasses and surfgrasses are ecosystem engineers on rocky shorelines where they show
41 remarkably high levels of primary production. Through analysis of their associated microbial
42 communities, we found a variety of microbial metabolisms that may benefit the host, including
43 nitrogen metabolisms and the production of B vitamins. In turn, these microbes have the genetic
44 capability to assimilate the dissolved organic compounds released by their phototroph hosts. We
45 describe a range of oxygen environments associated with surfgrass, including low-oxygen
46 microhabitats in their rhizomes that host genes for nitrogen fixation. The tremendous

47 productivity of coastal phototrophs is likely due in part to the activities of associated microbes
48 and an increased understanding of these associations is needed.

49

50 **Introduction**

51 We are experiencing a paradigm shift in biology with the recognition that many species exist as a
52 consortium with microbes (1). These microbial associations are nearly ubiquitous, spanning a
53 diversity of hosts across ecosystems. In coastal marine environments, phototrophic microbial
54 hosts are diverse and range from marine angiosperms to large eukaryotic protists (macroalgae).

55 Different macroalgal host species (2, 3) and different phototroph tissues (4, 5) host distinct
56 microbial communities numbering in the millions per cm² of host tissue (6), yet we still know
57 little about the functional role the microbiome plays in host fitness or how the host influences the
58 microbiome. The microbiome of phototroph species has been shown to have metabolisms that
59 provide nitrogen to the host (7, 8). Bacteria also supply B vitamins (9) and affect development of
60 their host (10). Further, the contributions that marine phototrophs make to host carbon and
61 nitrogen cycling have largely ignored the role that microbes play. Even as we begin to describe
62 their microbiome, we are discovering that environmental change affects these communities (11).
63 For many of the foundational phototrophic species in the coastal ocean, our understanding of the
64 diversity and role of their microbiome is nascent.

65

66 A unique aspect of host-associated microbes are the strong gradients in oxygen that they
67 experience due to the biological activities of the host. The photosynthetic and respiratory
68 activities of the host can generate a ‘phycosphere’ (12) where the host influences the physical
69 environment experienced by microbes, sometimes over micron or mm scales. For example, the

70 basal leaf meristem of the seagrass *Zostera* ranges from oxic to anoxic conditions over a scale of
71 300 microns when measured with oxygen microsensors (13). This range of oxygen
72 concentrations likely selects for a diversity of microbial metabolisms in association with
73 macrophytes.

74

75 Another factor important to the microbial metabolisms associated with coastal macrophytes is
76 nutrient availability. In coastal systems, nitrogen can limit primary production and microbial
77 associates that aid in accessing nitrogen might be selected. Microbial metabolisms that can
78 increase the available dissolved inorganic nitrogen (DIN) for the host (14) include pathways that
79 cleave carbon-nitrogen bonds to generate ammonium. This ammonification in biological systems
80 can result from a diversity of hydrolases, including ureases and other enzymes that cleave C-N
81 bonds (15). Further, microbes that fix atmospheric nitrogen have been discovered in an
82 increasing number of taxa (8, 16), now recognized to include heterotrophic as well as
83 phototrophic taxa (17–19). Nitrogen fixation was previously assumed to be restricted to nitrogen-
84 poor environments, but has been quantified recently in systems thought to be nitrogen-rich (8,
85 20), an enigmatic finding given that nitrogen fixation is a costly metabolic process that consumes
86 16 ATPs per N₂ fixed (21). Sediments where oxygen is low and nutrients can be depleted by
87 macrophytes, such as the rhizosphere of seagrasses have provided evidence of nitrogen fixation
88 (22–26). The recent discovery that nitrogen fixation takes place on particles in the coastal ocean
89 where nitrate is relatively abundant (8, 20) suggests that *nifH* genes could be abundant in other
90 nearshore systems.

91

92 Microbial metabolisms that synthesize compounds and vitamins needed by seaweeds and
93 seagrasses may also underlie host-microbe exchanges. The active form of Vitamin B1 (thiamin)
94 is essential for all organisms and is involved in carbohydrate and amino acid metabolisms.
95 Vitamin B2 (riboflavin)-binding proteins are co-enzymes in various oxidases and are involved in
96 photosynthesis and phototropism (27). Vitamin B7 (biotin) is a cofactor for acetyl coenzyme A
97 (coA) which is essential for fatty acid synthesis. Vitamin B12 (cobalamin) is required as a
98 coenzyme in the mitochondria for many algae, yet they depend upon prokaryotes to produce it
99 (9, 28). Thus, marine macrophytes may be auxotrophic for key vitamins, and their production by
100 host-associated bacteria may be another basis for phototroph-microbiome interactions in nature.
101
102 Hosts might reciprocally benefit microbes, especially if heterotrophic microbes benefit from the
103 dissolved organic carbon that is released by their hosts. Of the carbon that is fixed, kelp have
104 been demonstrated to release 15-16% of it as dissolved organic matter (29, 30), and seagrasses
105 too provide a constant source of dissolved organic carbon (31, 32), likely stimulating
106 heterotrophic bacterial processes (33). These rates of organic carbon release, often involving
107 highly labile organic carbon compounds (34), could provide the basis for reciprocal benefits
108 between microbes and their associated hosts.
109
110 Here, we analyzed microbial metagenomes collected from 5 different coastal phototrophs to
111 determine if there is functional genomic evidence of microbial metabolisms that could
112 reciprocally benefit host and microbes. We analyzed the surface microbiome on the blade of two
113 kelp species (*Laminaria setchellii* and *Nereocystis luetkeana*) and the surfgrass *Phyllospadix*
114 *scouleri*, the rhizomes of *P. scouleri*, *P. serrulatus*, and the seagrass species, *Zostera marina*, and

115 the sediment surrounding the rhizomes of *P. scouleri* and *Z. marina*. We quantified the variable
116 oxygen environment in the rhizomes of *Phyllospadix spp.* to determine if they allow for aerobic
117 as well as anaerobic metabolisms. We analyzed the microbial taxa present and examined their
118 gene content to estimate their functional and metabolic capacities. We hypothesized that
119 microbial partners: 1) enhance host access to dissolved inorganic nitrogen through nitrogen
120 recycling, ammonification and nitrogen fixation, 2) provision vitamins B₁, B₂, B₇, B₁₂, and 3) use
121 a diversity of abundant dissolved organic carbon exudates from the host. We tested whether
122 microbial taxonomy and function differed across hosts and host tissue types, and whether
123 anaerobic metabolisms were present in low-O₂ environments (e.g., rhizomes and sediment).
124 Through this study, we find that the range of oxygen environments engineered by host
125 phototrophs likely explains the diversity of both oxidizing and reducing microbial metabolisms,
126 and contributes to the functional capabilities of microbes and their influence on carbon and
127 nitrogen cycling in nearshore ecosystems.

128

129 **Methods**

130 *Sampling and DNA Extraction*

131 We collected metagenome samples from the surfaces of 5 different phototroph species (Table
132 S1). The surface of *Phyllospadix scouleri* blades, *Laminaria setchellii* fronds and the inner bulbs
133 of *Nereocystis luetkeana* were swabbed with a sterile swab and brushed with an interdental brush
134 (GUM Proxabrush Go-Betweens). We preserved sections of the rhizomes of *Phyllospadix*
135 *scouleri*, *P. serrulatus* and *Zostera marina*. Sediment surrounding *P. scouleri* and *Z. marina* was
136 also collected. All samples were collected from Tatoosh Island, WA, USA (48.393679, -
137 124.734617) on 16-17 Jul 2019, except for *Z. marina* samples which were sampled from West

138 Falmouth Bay, MA, USA (41.60708333, -70.64527778) on 19 Sept 2019. We included samples
139 from the rhizosphere of *Z. marina* from the Atlantic Ocean as a known positive control for
140 nitrogen fixation (22, 23). Swabs, tissue and sediment were immediately frozen at 20° C and
141 shipped to storage at -80° C. DNA from these collections was extracted with a Qiagen PowerSoil
142 Kit and multiple samples were pooled for each metagenome sample to increase DNA quantity
143 and possible discovery: *P. scouleri* blade, rhizome and sediment (3 pooled individuals each), *P.*
144 *serrulatus* rhizome (3 individuals), *L. setchellii* blade (3 individuals), *N. luetkeana* interior bulb
145 (4 individuals), *Z. Marina* rhizomes and sediment (2 individuals).

146

147 *Shotgun metagenomic sequencing, assembly, and read recruitment*

148 The above 8 samples were run over 2 lanes on a HiSeq 2500 (2x150) with TruSeq DNA library
149 preps at Argonne National Laboratory. For each sample, resulting DNA sequences were first
150 quality filtered (35)(Minoche et al. 2011), then assembled with IDBA-UD v1.1.3 (36) (Peng et
151 al. 2012) with a minimum scaffold length of 1 kbp. Metagenomic short reads from each sample
152 were then recruited back to their corresponding assembled contigs using Bowtie2 (37). Samtools
153 (38) was used to generate sorted and indexed BAM files. Anvi'o v7.0 (39) was used as the
154 command line environment for all downstream analyses. ‘anvi-gen-contigs-database’ was used
155 to generate anvi’o contigs databases, during which Prodigal v2.6.3 (40) identified open reading
156 frames, and ‘anvi-run-hmms’ was used to identify genes matching to archaeal and bacterial
157 single-copy core gene collections using HMMER (41).

158

159 *Reconstructing metagenome-assembled genomes (MAGs)*

160 To reconstruct genomes from the assembled metagenomes, we used a combination of automatic
161 binning via CONCOCT v1.1.0 (42), followed by a manual curation of each MAG as outlined by
162 Shaiber et al. 2020 (43). Genome taxonomy was determined using GTDB v.1.3.0 (44), and 'anvi-
163 run-scg-taxonomy'. We also inferred gene-level taxonomy using Centrifuge v1.0.4 (45) to aid
164 manual curation.

165

166 *Phylogenomic analysis of MAGs*

167 To perform a phylogenomic analysis of our MAGs, we recovered amino acid sequences for
168 bacterial single-copy core genes (SCGs) from each genome (except the only archaeal genome in
169 our collection) using the program 'anvi-get-sequences-for-hmm-hits' with the parameter '--
170 hmm-source 'Bacteria_71' on the ribosomal gene set 'Ribosomal L1-L6' and the flag '--
171 concatenate', which independently aligned each SCG independently using Muscle v3.8.1 (46)
172 before concatenating them into a final superalignment. We then refined the alignment using
173 trimAl v1.4.rev15 (47) to remove any position in the alignment if more than 50% of the residues
174 were gap characters. A maximum-likelihood phylogeny was inferred using IQTree (48) with
175 1,000 bootstrap replicates, and a LG+R6 model best fit our data using ModelFinder (49).

176

177 *Functional analysis of microbial communities*

178 To address the metabolic capabilities of host-associated microbes, we annotated genes in each
179 anvi'o contigs database with 3 different databases using 'anvi-run-kegg-kofams', 'anvi-run-ncbi-
180 cogs', and 'anvi-run-pfams', which used the databases of Kyoto Encyclopedia of Genes and
181 Genomes (KEGG) (50), NCBI's Clusters of Orthologous Genes (COGs) (51) and EBI's Pfam
182 database (52) respectively. We used these annotated genes to test for 1) nitrogen cycling

183 metabolisms, especially those within the nitrogen-fixation pathway, 2) hydrolases, including
184 ureases, as well as ammonia-lyases, to cleave the C-N bonds in amino acids and make
185 ammonium available to the host, 3) vitamin production, namely vitamins B₁, B₂, B₇ and B₁₂ and
186 4) a set of dissolved organic matter (DOM) transporter genes identified by Poretsky et al. (34)
187 that indicate the ability of the microbial community to assimilate DOM exudates from kelps and
188 surfgrasses. The list of genes used is indicated in Table S4. We additionally developed and used
189 a graph-based algorithm on KEGG definitions for vitamins B₁, B₂, B₇ and B₁₂ to detect the
190 presence of these biosynthetic pathways (Supplementary Code 1). To expand our functional
191 analysis of kelp blade genes, we included 32 MAGs from the surface of *N. luetkeana* blades that
192 were collected from the same location at the same time using similar methods as those described
193 above (53).

194

195 *Phylogenetic analysis of nifH genes*

196 To search for *nifH* amino acid sequences in our environmental samples, we identified 9 MAGs
197 which contained *nifH* genes using the KEGG identifier K02588 with e-value < 1e-20. We
198 aligned the AA sequences for these genes against 89 well-characterized reference *nifH* AA
199 sequences (Table S6) using Muscle v3.8.1 (46) and refined the alignment using trimAl (gap-
200 threshold: 0.5) and ‘anvi-script-reformat-fasta’ (max-percentage-gap: 50%). A maximum-
201 likelihood phylogeny was inferred using IQTree (48) with 1,000 bootstrap replicates, and a
202 LG+R5 model best fit our data using ModelFinder (49). *nifH* genes from the *Zostera* samples
203 served as positive controls to detect nitrogen fixation genes in other samples. Figures 2, 3, 4 were
204 generated using iTol v5 (54), R v4.0.3 and FigTree respectively. We additionally took tissue
205 samples from *P. scouleri* rhizome (n = 16), basal meristematic region just distal to the sheath

206 (n = 12) and blade 35 cm above the rhizome (n = 12) to quantify stable isotopes of $\delta^{15}\text{N}$ and
207 $\delta^{13}\text{C}$ to look for signatures of nitrogen fixation (methods described in Appendix 1).

208

209 *Quantifying the Oxygen Environment*

210 We quantified the oxygen concentrations in proximity to *Phyllospadix spp.* rhizomes by
211 comparing dissolved oxygen (DO) concentrations in the surrounding seawater and in the
212 sediment around the rhizome. We used a Pyro Science Robust Oxygen Probe (OXROB10,
213 Firesting™, Pyroscience), and repeated measurements around 0900h across 4 days (7-9 June
214 2019, 13 June 2021) within *P. scouleri* (n = 18) and *P. serrulatus* (n = 11) rhizomes. Each
215 reading first measured the surrounding seawater after which we gently pushed the tip of the
216 oxygen probe into the sediment and rhizome mass to a depth of 1-3 mm, the typical thickness
217 (*pers. observation*). We let the probe equilibrate and took a reading at 150 sec. This allowed the
218 rhizome oxygen environment to equilibrate after we disturbed the intact rhizome. We compared
219 surrounding water and within-rhizome oxygen using paired t-tests in R.

220

221 *Data Availability*

222 In addition to the code available on GitHub (____), the final MAG database files generated in
223 anvi'o are available on the FigShare repository: (____). Metagenomic sequence data are
224 available at the NCBI's Sequence Read Archive under accession no. (submission in progress).

225

226 **Results**

227 *Surfgrass rhizomes have lower oxygen concentrations than surrounding seawater*

228 The oxygen environment in the rhizomes differed significantly from that of the surrounding
229 seawater (Fig. 1). Rhizomes maintained a lower dissolved oxygen (DO) concentration than the
230 surrounding seawater for both *P. scouleri* (n=18, pairwise t-test: $p<0.001$) and *P. serrulatus*
231 (n=11, pairwise t-test: $p<0.001$). *P. serrulatus* maintained a slightly lower DO concentration in
232 the rhizome at 2.11 mg l^{-1} , compared to 5.61 mg l^{-1} for *P. scouleri*. However, the nature of
233 sampling likely introduced more oxygenated water from the surrounding water column to the
234 rhizome-sediment microenvironment, suggesting that the actual DO concentration within the
235 sediment is lower than the value reported.

236

237 *Diversity of MAGs assembled across hosts*

238 Following filtering, we obtained an average of 41 million reads per sample (range 6.48 to 67.73
239 million), with 79.8% of raw reads retained on average. When these reads were assembled into
240 contigs of at least 1000 nucleotides, a mean of 42,026 contigs and a mean of 110,054 genes were
241 present across samples (Table S1).

242

243 Across 8 metagenomes we manually binned 33 high quality MAGs, defined as having a
244 completion score $>90\%$ and contamination (or redundancy) $< 10\%$ (Table 2). We also identified
245 39 lower quality MAGs that had completion scores between 38 and 93% and redundancy scores
246 between 0 and 21% (Table S3). All MAGs were bacterial except for a single archaeal MAG on
247 the rhizome of *P. scouleri*. The bacterial MAGs spanned 7 phyla, including *Proteobacteria*
248 (n=34), *Bacteroidota* (n=19), *Verrumicrobia* (n=2), *Campylobacterota* (n=3), *Desulfobacterota*
249 (n=5), and a single MAG in each of *Desulfomonadota*, *Acidobacteriota*, and *Spirochaetota*. The
250 Archaea belonged to the phylum *Chrenarchaeota*. There were 46 MAGs resolved to the species

251 level, with 8 to the genus level, 9 to family, 2 to order, and 2 to class level. Five MAGs were
252 resolved only as Bacteria (Table S2).

253
254 The 72 MAGs belong to diverse microbial phyla, which were distributed across the 5 host
255 species and tissue types (Fig. 2). In some cases, bacterial taxa from kelp blade tissues were most
256 closely related to bacteria collected from the rhizome or sediment of a seagrass, suggesting that
257 closely related bacterial taxa can associate with diverse hosts. Known anaerobic sulfur cyclers
258 like *Desulfobulbia*, *Desulfobacteria*, *Desulfuromonadia* and *Campylobacteria* (*Sulfurovum*
259 *sp000296775* and *Sulfurimonas autotrophica*) were exclusively found in the low oxygen rhizome
260 and sediment samples of *Zostera marina* and *Phyllospadix* spp. Conversely,
261 *Alphaproteobacteria*, were exclusively found on surfaces exposed to the water column.
262 *Gammaproteobacteria* was the only class found across the range of tissue types (6 out of 8 host
263 environments). We did not include the only well-resolved archaeal taxon found in our samples,
264 *Crenarchaea* (*P. scouleri* rhizome), as our analysis compared single-copy core genes specific to
265 bacterial phyla.

266
267 *Host-associated microbial genomes contain pathways to synthesize vitamins, recycle nitrogen,*
268 *and use host-generated carbon*
269 We found evidence for a number of metabolic pathways that are likely important for exchanges
270 between host phototrophs and their microbial partners (Fig. 3). Microbes on hosts had genes for
271 diverse carbohydrate and carboxylic acid assimilation via cell membrane transport proteins.
272 Host-associated microbes also had genes for a diversity of nitrogen metabolisms, including
273 ureases and hydrolases that could regenerate ammonium. Nitrogen metabolisms were most

274 diverse in rhizome and sediment samples where we identified both oxidizing (nitrification) and
275 reducing (nitrate reduction, nitrogen fixation, denitrification) metabolisms, as well as
276 metabolisms that both oxidize and reduce (annamox).

277

278 Every sample had at least one gene from B-vitamins biosynthesis pathways. Using a simple-path
279 based algorithm on KEGG definitions (Supplementary Code 1), we determined that all microbial
280 communities had the metabolic pathways to synthesize vitamins B₁ (with the exception of the *P.*
281 *scouleri* rhizome), B₂ and B₇ (except inside the bulb of *N. luetkeana*). The Vitamin B₁₂ anaerobic
282 biosynthesis pathway, however, was only present in MAGs found on the blades of *L. setchellii*
283 (2) and *P. scouleri* (3) and the rhizomes of *P. serrulatus* (2) and *Z. marina* (1). Additionally, all
284 three MAGs on the blade of *P. scouleri* that had this anaerobic pathway had the genes necessary
285 to synthesize Vitamin B₁₂ aerobically as well.

286

287 *Novel detection of nifH genes in surfgrass*

288 We identified the nitrogenase gene (*nifH*) in 9 MAGs with e-value support < 1.3e-120 (KEGG)
289 and < 1.1e-135 (COG). These 9 MAGs were assembled from *P. serrulatus* rhizomes (n = 2) and
290 *Z. marina* rhizomes (n = 3) and the surrounding sediment (n = 4). Of these 9 MAGs, 5 were
291 resolved to the genus level, while others were resolved to the order and family level, including
292 *Campylobacteriales*, *Desulfobacteriales* and 2 *Flavobacteriaceae* (Fig. 4, Table S5). *nifH* genes
293 identified in the rhizomes of *P. serrulatus* and *Z. marina* belonging to the class *Desulfobacteria*
294 and family *Flavobacteriaceae*, clustered within Cluster III: anaerobic nitrogen-fixers that are
295 often coupled with sulfate-reduction metabolisms. Samples from *Z. marina* sediment and
296 rhizome also contained 3 *nifH* genes in *Campylobacterial* MAGs that clustered together in a

297 sister clade to the aerobic nitrogen-fixers of Cluster I. The COG gene identified as *nifH*
298 (COG1348) also includes the homologous protochlorophyllides, which are involved in
299 photosynthetic pigment synthesis but have high sequence similarity to the *nifH* gene (21, 55).
300 Instead, we used the KEGG gene (K02588) that does not detect these homologs. When we
301 inspected genes on the same contig with *nifH*, we found a number of genes related to nitrogen
302 fixation (Table S5), including *nifD* (COG 2710) in 7 of the 9 contigs, nitrogen regulatory protein
303 PII (COG 347), *nifB* (COG 535), and multiple iron containing proteins including ferrodoxin and
304 Fe-Mo cluster-binding proteins (Table S5).

305

306

Discussion

307 *Phototroph tissues and sediment host distinct microbial taxa and functions*

308 The phototroph species we sampled in this study are foundational in coastal ecosystems (56–59),
309 yet a description of the diversity and function of their microbiomes have been lacking. All
310 MAGs were bacterial, except for a single archaeal MAG (*Crenarchaeota*) in the rhizome of
311 *Phyllospadix scouleri*, which was identified as *Nitrosopumulis*, a genus associated with
312 nitrification (Table S3). Together, these 5 phototrophs hosted bacteria from 9 phyla. The only
313 low diversity sample was the interior of the bulb of *Nereocystis*, where we assembled only a
314 single MAG (*UBA7415 sp002470515*) suggesting that this environment of high carbon
315 monoxide and nitrogen gas (60) may inhibit microbial activity or pose a highly selective
316 environment. Blades of kelp and surfgrass, in contrast, were a locus of microbial diversity and
317 function, a finding that is similar to many recent studies of macroalgal and seagrass microbiomes
318 reporting high microbial diversity (2, 4, 5, 61–63). The functional attributes of microbial taxa
319 associated with marine macrophytes include pathogen resistance (64), the ability to provision the

320 host with B vitamins (9), and enhanced host algal fitness (65), perhaps through some of the
321 nitrogen metabolisms we documented here (14, 66).

322

323 *Host-microbe interactions in a dynamic oxygen microenvironment*

324 Grouping MAGs by microbial metabolisms (Fig. 3) showed key functional differences among
325 phototroph hosts. Blade tissues that interacted directly with the water column were associated
326 with microbial nitrogen metabolisms that were mostly oxidizing. The abundance of dissolved
327 organic carbon from phototroph hosts (29–31, 59) might select for heterotrophic metabolisms.
328 Indeed, we found an abundance of genes for dissolved organic matter assimilation and transport
329 in all metagenomes, suggesting that hosts may stimulate heterotrophy in their associated
330 microbial community similar to findings by Poretsky et al. (34). Improved characterization of the
331 components of dissolved organic matter and the genomes of hosts will allow us to better assess
332 complementarity in resource supply by hosts and resource use by microbes.

333

334 The host tissue types in this study differed in surface oxygen concentrations. Blade tissue
335 interacts with the water column and is likely more oxygenated than rhizome tissue or sediments,
336 though a previous study suggests there can also be a 60% reduction in oxygen along the
337 immediate surface of kelp blades (67), and along the mucus layer where some kelp-associated
338 bacteria reside (6). Over two-thirds of the bacterial taxa on blades of *N. luetkeana* belonged to
339 families associated with obligately aerobic metabolisms, demonstrating the role of oxygen in
340 shaping phototroph-associated microbial communities (68). The sediment surrounding the
341 rhizomes of *Phyllospadix spp.* contained low oxygen microenvironments (Fig. 1) likely
342 maintained by macroinvertebrate respiration (69)(Moulton and Hacker 2011), similar to the

343 biological processes in the anaerobic sediment surrounding *Zostera* (13). Low rhizosphere
344 oxygen concentrations likely structured the taxonomic composition of *Z. marina* to include
345 anaerobic taxa such as *Campylobacteria*, *Desulfatitalea* and *Desulfobulbus*. The presence of
346 anaerobes like *Desulfuromonadia*, *Desulfobacteria*, *Spirochaeta* and *Aminicenania* in *P.*
347 *serrulatus* rhizomes suggests sulfate reduction also occurs, possibly coupled to dissolved organic
348 carbon use as an energy source (e.g. (70) Howarth & Hobbie 1982). Additionally,
349 *Campylobacteria* and the genus *Thiodiazotropha* were associated with *Z. marina* and may
350 remove detrimental sulfide accumulation through sulfur oxidation (71, 72).

351
352 Nitrogen metabolisms that were both oxidizing and reducing were found in MAGs associated
353 with rhizomes of both *Z. marina* and *Phyllospadix* (Fig. 3), suggesting the potential for temporal
354 niches when, for example, ammonium oxidation to nitrate occurs during high-O₂ daylight
355 periods, followed by nitrate reduction or nitrogen fixation during O₂-depleted nighttime hours.
356 Additionally, all MAGs in this study contained hydrolases that cleave carbon-nitrogen bonds to
357 produce ammonium (14), recycling nitrogen compounds for host uptake. Oxidizing and reducing
358 metabolisms are likely separated only by microns in the hosts studied here.

359
360 We detected biosynthetic pathways for vitamins B₁, B₂, B₇ and B₁₂ that are required by the
361 auxotrophic phototroph hosts in this study (9, 10, 73). We found that only the blades of *P.*
362 *scouleri* harbored MAGs with both anaerobic and aerobic biosynthetic pathways for Vitamin
363 B₁₂, suggesting that the variable oxygen environment driven by host-metabolism creates diverse
364 metabolic niches for associated microbes. Strong gradients in oxygen and metabolically diverse
365 microbial metabolisms are present in a diversity of animal hosts such as corals and sponges as a

366 result of host metabolism (74–76). Fluctuating oxygen microenvironments might also promote
367 cross-feeding, where microbial taxa produce a metabolite that can be consumed by other taxa.
368 Cross-feeding is potentially important for nitrogen (77) and carbon metabolisms (78, 79) in
369 microbial communities.

370

371 *Characteristics of previously undescribed nitrogen fixation in surfgrass*

372 Building on recent studies that illustrate the association of nitrogen fixing microbes with a
373 diversity of macroalgae (80) and seagrasses (22, 23, 81, 82), we found a previously undescribed
374 diversity of nitrogenase genes associated with the surfgrass *Phyllospadix*. We detected *nifH*
375 genes in *P. serrulatus* rhizomes that resolved into the Cluster I group of *nifH* genes, which are
376 characterized by aerobic nitrogen fixers. *P. serrulatus*, in comparison to *P. scouleri*, is found
377 higher up in the intertidal zone and often in sheltered tidepools that tend to undergo dramatic
378 daily fluctuations in oxygen, possibly allowing for a temporal low-O₂ niche during the night
379 (83). Conversely, we did not detect nitrogenase genes in the microbiome of *P. scouleri*, which
380 inhabits more wave-exposed and thus better oxygenated environments (Fig. 1). However, stable
381 isotope analyses across *P. scouleri* samples show a lower nitrogen isotopic signature in the
382 rhizome compared to the rest of the plant, a possible indication of nitrogen from an atmospheric
383 source (Fig. S1), though *in situ* experiments with stable isotope tracers are needed to confirm the
384 presence of nitrogen fixation.

385

386 Nitrogen fixation by microbial associates provides a key means of increasing the availability of
387 ammonium, possibly supporting primary productivity. *P. scouleri* biomass reaches 12.7 kg of
388 wet mass per square meter of shore and exudes 0.93 mg C per hour per gram dry mass as

389 dissolved organic carbon that may fuel microbial activity (59). There is evidence that nitrogen
390 fixation can contribute to seagrass productivity (66, 84), a possible adaptation to low nitrogen
391 environments. Our finding that nitrogen fixing microbes are associated with a rocky intertidal
392 surfgrass is especially surprising given that Tatoosh Island is in an area of upwelling and high
393 DIN (86) at the more northerly end of the California Current Large Marine Ecosystem. Whether
394 nitrogen fixation forms the basis for reciprocal host-microbe exchange is still unknown.

395

396 The metagenomic analyses we present here suggest that phototroph-associated microbiomes may
397 be involved in carbon, nitrogen and vitamin metabolisms important to their hosts, likely
398 generating commensal or mutualistic interactions. Future experiments should test these
399 hypothesized interactions between host and microbiome. The importance of seaweeds and
400 seagrasses to coastal productivity, and the demonstrated sensitivity of both host and microbes to
401 increasing temperatures and pH (11, 62, 85), pathogens (61), and other anthropogenic stressors,
402 underline the importance of further studying phototroph-microbiome interactions.

403

404 **Acknowledgements**

405 Our gratitude to the Makah Tribal Nation for access to Tatoosh Island. We thank The University
406 of Chicago's Microbiome Center for pilot award funding, and Washington Department of
407 Natural Resources grants 93099282, 93100399 (CAP) and NSF-DEB grant (#1556874) awarded
408 to JT Wootton. We appreciate the work of C Saucedo in the isotope analysis, and A Wootton, A
409 Wood and K Foreman in the field sampling. KM was supported by an EE Fellowship from The
410 University of Chicago. S Owens and S Greenwald at Argonne National Lab provided expertise
411 in sequencing.

412

References

413 1. McFall-Ngai M, Hadfield MG, Bosch TCG, Carey HV, Domazet-Lošo T, Douglas AE,
414 Dubilier N, Eberl G, Fukami T, Gilbert SF, Hentschel U, King N, Kjelleberg S, Knoll AH,
415 Kremer N, Mazmanian SK, Metcalf JL, Nealon K, Pierce NE, Rawls JF, Reid A, Ruby EG,
416 Rumpho M, Sanders JG, Tautz D, Wernegreen JJ. 2013. Animals in a bacterial world, a new
417 imperative for the life sciences. *Proc Natl Acad Sci USA* 110:3229–3236.

418 2. Weigel BL, Pfister CA. 2019. Successional Dynamics and Seascape-Level Patterns of
419 Microbial Communities on the Canopy-Forming Kelps *Nereocystis luetkeana* and *Macrocystis*
420 *pyrifera*. *Frontiers in Microbiology* 10:346.

421 3. Lemay MA, Martone PT, Keeling PJ, Burt JM, Krumhansl KA, Sanders RD, Wegener
422 Parfrey L. 2018. Sympatric kelp species share a large portion of their surface bacterial
423 communities: Kelp-associated bacterial diversity. *Environmental Microbiology* 20:658–670.

424 4. Quigley CTC, Capistrant-Fossa KA, Morrison HG, Johnson LE, Morozov A, Hertzberg
425 VS, Brawley SH. 2020. Bacterial Communities Show Algal Host (*Fucus* spp.)/Zone
426 Differentiation Across the Stress Gradient of the Intertidal Zone. *Front Microbiol* 11:563118.

427 5. Lemay MA, Davis KM, Martone PT, Parfrey LW. 2021. Kelp-associated Microbiota are
428 Structured by Host Anatomy¹. *J Phycol* 57:1119–1130.

429 6. Ramirez-Puebla ST, Weigel BL, Jack L, Schlundt C, Pfister CA, Mark Welch JL. 2020.
430 Spatial organization of the kelp microbiome at micron scales. preprint, *Microbiology*.

431 7. Jacoby R, Peukert M, Succurro A, Koprivova A, Kopriva S. 2017. The Role of Soil
432 Microorganisms in Plant Mineral Nutrition—Current Knowledge and Future Directions. *Front*
433 *Plant Sci* 8:1617.

434 8. Mills MM, Turk-Kubo KA, van Dijken GL, Henke BA, Harding K, Wilson ST, Arrigo

435 KR, Zehr JP. 2020. Unusual marine cyanobacteria/haptophyte symbiosis relies on N₂ fixation
436 even in N-rich environments. *The ISME Journal* <https://doi.org/10.1038/s41396-020-0691-6>.

437 9. Croft MT, Lawrence AD, Raux-Deery E, Warren MJ, Smith AG. 2005. Algae acquire
438 vitamin B12 through a symbiotic relationship with bacteria. *Nature* 438:90–93.

439 10. Wichael T, Charrier B, Mineur F, Bothwell JH, Clerck OD, Coates JC. 2015. The green
440 seaweed *Ulva*: a model system to study morphogenesis. *Front Plant Sci* 6.

441 11. Qiu Z, Coleman MA, Provost E, Campbell AH, Kelaher BP, Dalton SJ, Thomas T,
442 Steinberg PD, Marzinelli EM. 2019. Future climate change is predicted to affect the microbiome
443 and condition of habitat-forming kelp. *Proceedings of the Royal Society B: Biological Sciences*
444 286:20181887.

445 12. Bell W, Mitchell R. 1972. Chemotactic and Growth Responses of Marine Bacteria to
446 Algal Extracellular Products. *Biological Bulletin* 143:265–277.

447 13. Brodersen KE, Siboni N, Nielsen DA, Pernice M, Ralph PJ, Seymour J, Kühl M. 2018.
448 Seagrass rhizosphere microenvironment alters plant-associated microbial community
449 composition. *Environ Microbiol* 20:2854–2864.

450 14. Tarquinio F, Bourgouin J, Koenders A, Laverock B, Säwström C, Hyndes GA. 2018.
451 Microorganisms facilitate uptake of dissolved organic nitrogen by seagrass leaves. *The ISME
452 Journal* <https://doi.org/10.1038/s41396-018-0218-6>.

453 15. Ladd JN, Jackson RB. 1982. Biochemistry of Ammonification, p. 173–228. *In* Stevenson,
454 FJ (ed.), *Agronomy Monographs*. American Society of Agronomy, Crop Science Society of
455 America, Soil Science Society of America, Madison, WI, USA.

456 16. Delmont TO, Quince C, Shaiber A, Esen ÖC, Lee ST, Rappé MS, McLellan SL, Lücker
457 S, Eren AM. 2018. Nitrogen-fixing populations of Planctomycetes and Proteobacteria are

458 abundant in surface ocean metagenomes. *Nature Microbiology* 3:804–813.

459 17. Sohm JA, Webb EA, Capone DG. 2011. Emerging patterns of marine nitrogen fixation.

460 *Nat Rev Microbiol* 9:499–508.

461 18. Bombar D, Paerl RW, Riemann L. 2016. Marine Non-Cyanobacterial Diazotrophs:

462 Moving beyond Molecular Detection. *Trends in Microbiology* 24:916–927.

463 19. Harding K, Turk-Kubo KA, Sipler RE, Mills MM, Bronk DA, Zehr JP. 2018. Symbiotic

464 unicellular cyanobacteria fix nitrogen in the Arctic Ocean. *Proc Natl Acad Sci USA* 115:13371–

465 13375.

466 20. Cabello AM, Turk-Kubo KA, Hayashi K, Jacobs L, Kudela RM, Zehr JP. 2020.

467 Unexpected presence of the nitrogen-fixing symbiotic cyanobacterium UCYN-A in Monterey

468 Bay, California. *J Phycol* 56:1521–1533.

469 21. Raymond J, Siefert JL, Staples CR, Blankenship RE. 2004. The Natural History of

470 Nitrogen Fixation. *Molecular Biology and Evolution* 21:541–554.

471 22. Patriquin D, Knowles R. 1972. Nitrogen fixation in the rhizosphere of marine

472 angiosperms. *Marine Biology* 16:49–58.

473 23. Capone DG. 1982. Nitrogen Fixation (Acetylene Reduction) by Rhizosphere Sediments

474 of the Eelgrass *Zostera marina*. *Marine Ecology Progress Series* 10:67–75.

475 24. Cole L, McGlathery K. 2012. Nitrogen fixation in restored eelgrass meadows. *Marine*

476 *Ecology Progress Series* 448:235–246.

477 25. Agawin N, Ferriol P, Sintes E. 2019. Simultaneous measurements of nitrogen fixation in

478 different plant tissues of the seagrass *Posidonia oceanica*. *Mar Ecol Prog Ser* 611:111–127.

479 26. Aoki L, McGlathery K. 2019. High rates of N fixation in seagrass sediments measured

480 via a direct $^{30}\text{N}_2$ push-pull method. *Mar Ecol Prog Ser* 616:1–11.

481 27. Massey V. 2000. The chemical and biological versatility of riboflavin. 28:283–296.

482 28. Grossman A. 2016. Nutrient Acquisition: The Generation of Bioactive Vitamin B 12 by
483 Microalgae. *Current Biology* 26:R319–R321.

484 29. Reed DC, Carlson CA, Halewood ER, Nelson JC, Harrer SL, Rassweiler A, Miller RJ.
485 2015. Patterns and controls of reef-scale production of dissolved organic carbon by giant kelp *M*
486 *acrocystis pyrifera*: DOC production by giant kelp. *Limnology and Oceanography* 60:1996–
487 2008.

488 30. Weigel BL, Pfister CA. 2021. The dynamics and stoichiometry of dissolved organic
489 carbon release by kelp. *Ecology* 102.

490 31. Wetzel RG, Penhale PA. 1979. Transport of carbon and excretion of dissolved organic
491 carbon by leaves and roots/rhizomes in seagrasses and their epiphytes. *Aquatic Botany* 6:149–
492 158.

493 32. Barrón C, Apostolaki ET, Duarte CM. 2014. Dissolved organic carbon fluxes by seagrass
494 meadows and macroalgal beds. *Frontiers in Marine Science* 1.

495 33. Pfister CA, Altabet MA. 2019. Enhanced microbial nitrogen transformations in
496 association with macrobiota from the rocky intertidal. *Biogeosciences* 16:193–206.

497 34. Poretsky RS, Sun S, Mou X, Moran MA. 2010. Transporter genes expressed by coastal
498 bacterioplankton in response to dissolved organic carbon. *Environmental Microbiology* 12:616–
499 627.

500 35. Minoche AE, Dohm JC, Himmelbauer H. 2011. Evaluation of genomic high-throughput
501 sequencing data generated on Illumina HiSeq and Genome Analyzer systems. *Genome Biol*
502 12:R112.

503 36. Peng Y, Leung HCM, Yiu SM, Chin FYL. 2012. IDBA-UD: a de novo assembler for

504 504 single-cell and metagenomic sequencing data with highly uneven depth. *Bioinformatics*
505 505 28:1420–1428.

506 506 37. Langmead B, Salzberg SL. 2012. Fast gapped-read alignment with Bowtie 2. *Nat*
507 507 *Methods* 9:357–359.

508 508 38. Li H, Handsaker B, Wysoker A, Fennell T, Ruan J, Homer N, Marth G, Abecasis G,
509 509 Durbin R, 1000 Genome Project Data Processing Subgroup. 2009. The sequence alignment/map
510 510 format and SAMtools. *Bioinformatics* 25:2078–2079.

511 511 39. Eren AM, Kiefl E, Shaiber A, Veseli I, Miller SE, Schechter MS, Fink I, Pan JN, Yousef
512 512 M, Fogarty EC, Trigodet F, Watson AR, Esen ÖC, Moore RM, Clayssen Q, Lee MD, Kivenson
513 513 V, Graham ED, Merrill BD, Karkman A, Blankenberg D, Eppley JM, Sjödin A, Scott JJ,
514 514 Vázquez-Campos X, McKay LJ, McDaniel EA, Stevens SLR, Anderson RE, Fuessel J,
515 515 Fernandez-Guerra A, Maignien L, Delmont TO, Willis AD. 2021. Community-led, integrated,
516 516 reproducible multi-omics with anvi'o. *Nat Microbiol* 6:3–6.

517 517 40. Hyatt D, Chen G-L, LoCascio PF, Land ML, Larimer FW, Hauser LJ. 2010. Prodigal:
518 518 prokaryotic gene recognition and translation initiation site identification. *BMC Bioinformatics*
519 519 11:119.

520 520 41. Eddy SR. 2011. Accelerated Profile HMM Searches. *PLoS Comput Biol* 7:e1002195.

521 521 42. Alneberg J, Bjarnason BS, de Bruijn I, Schirmer M, Quick J, Ijaz UZ, Lahti L, Loman
522 522 NJ, Andersson AF, Quince C. 2014. Binning metagenomic contigs by coverage and composition.
523 523 *Nat Methods* 11:1144–1146.

524 524 43. Shaiber A, Willis AD, Delmont TO, Roux S, Chen L-X, Schmid AC, Yousef M, Watson
525 525 AR, Lolans K, Esen ÖC, Lee STM, Downey N, Morrison HG, Dewhirst FE, Mark Welch JL,
526 526 Eren AM. 2020. Functional and genetic markers of niche partitioning among enigmatic members

527 of the human oral microbiome. *Genome Biol* 21:292.

528 44. Parks DH, Chuvochina M, Rinke C, Mussig AJ, Chaumeil P-A, Hugenholtz P. 2021.

529 GTDB: an ongoing census of bacterial and archaeal diversity through a phylogenetically

530 consistent, rank normalized and complete genome-based taxonomy. *Nucleic Acids Research*

531 gkab776.

532 45. Kim D, Song L, Breitwieser FP, Salzberg SL. 2016. Centrifuge: rapid and sensitive

533 classification of metagenomic sequences. *Genome Res* 26:1721–1729.

534 46. Edgar RC. 2004. MUSCLE: multiple sequence alignment with high accuracy and high

535 throughput. *Nucleic Acids Research* 32:1792–1797.

536 47. Capella-Gutierrez S, Silla-Martinez JM, Gabaldon T. 2009. trimAl: a tool for automated

537 alignment trimming in large-scale phylogenetic analyses. *Bioinformatics* 25:1972–1973.

538 48. Nguyen L-T, Schmidt HA, von Haeseler A, Minh BQ. 2015. IQ-TREE: A Fast and

539 Effective Stochastic Algorithm for Estimating Maximum-Likelihood Phylogenies. *Molecular*

540 *Biology and Evolution* 32:268–274.

541 49. Kalyaanamoorthy S, Minh BQ, Wong TKF, von Haeseler A, Jermiin LS. 2017.

542 ModelFinder: fast model selection for accurate phylogenetic estimates. *Nat Methods* 14:587–

543 589.

544 50. Kanehisa M. 2000. KEGG: Kyoto Encyclopedia of Genes and Genomes. *Nucleic Acids*

545 *Research* 28:27–30.

546 51. Galperin MY, Makarova KS, Wolf YI, Koonin EV. 2015. Expanded microbial genome

547 coverage and improved protein family annotation in the COG database. *Nucleic Acids Research*

548 43:D261–D269.

549 52. Mistry J, Chuguransky S, Williams L, Qureshi M, Salazar GA, Sonnhammer ELL,

550 550 Tosatto SCE, Paladin L, Raj S, Richardson LJ, Finn RD, Bateman A. 2021. Pfam: The protein
551 families database in 2021. *Nucleic Acids Research* 49:D412–D419.

552 53. Weigel BL, Miranda KK, Fogarty EC, Watson AR, Pfister CA. in review. Functional
553 insights into the kelp microbiome from metagenome assembled genomes.

554 54. Letunic I, Bork P. 2021. Interactive Tree Of Life (iTOL) v5: an online tool for
555 phylogenetic tree display and annotation. *Nucleic Acids Research* 49:W293–W296.

556 55. Kapili BJ, Dekas AE. 2021. PPIT: an R package for inferring microbial taxonomy from
557 *nifH* sequences. *Bioinformatics* 37:2289–2298.

558 56. Shelton AO. 2010. Temperature and community consequences of the loss of foundation
559 species: Surfgrass (*Phyllospadix* spp., Hooker) in tidepools. *Journal of Experimental Marine
560 Biology and Ecology* 391:35–42.

561 57. Lefcheck JS, Wilcox DJ, Murphy RR, Marion SR, Orth RJ. 2017. Multiple stressors
562 threaten the imperiled coastal foundation species eelgrass (*Zostera marina*) in Chesapeake Bay,
563 USA. *Glob Change Biol* 23:3474–3483.

564 58. Pfister CA, Altabet MA, Weigel BL. 2019. Kelp beds and their local effects on seawater
565 chemistry, productivity, and microbial communities. *Ecology* <https://doi.org/10.1002/ecy.2798>.

566 59. Miranda KK, Weigel BL, McCoy SJ, Pfister CA. 2021. Differential impacts of alternate
567 primary producers on carbon cycling. *Ecology* <https://doi.org/10.1002/ecy.3455>.

568 60. Liggan LM, Martone PT. 2018. Under pressure: biomechanical limitations of developing
569 pneumatocysts in the bull kelp (*Nereocystis luetkeana*, Phaeophyceae). *Journal of Phycology*
570 54:608–615.

571 61. Egan S, Harder T, Burke C, Steinberg P, Kjelleberg S, Thomas T. 2013. The seaweed
572 holobiont: understanding seaweed–bacteria interactions. *FEMS Microbiology Reviews* 37:462–

573 476.

574 62. Minich JJ, Morris MM, Brown M, Doane M, Edwards MS, Michael TP, Dinsdale EA.

575 2018. Elevated temperature drives kelp microbiome dysbiosis, while elevated carbon dioxide

576 induces water microbiome disruption. PLOS ONE 13:e0192772.

577 63. Capistrant-Fossa KA, Morrison HG, Engelen AH, Quigley CTC, Morozov A, Serrão EA,

578 Brodie J, Gachon CMM, Badis Y, Johnson LE, Hoarau G, Abreu MH, Tester PA, Stearns LA,

579 Brawley SH. 2021. The microbiome of the habitat-forming brown alga *Fucus vesiculosus*

580 (Phaeophyceae) has similar cross-Atlantic structure that reflects past and present drivers ¹. J

581 Phycol jpy.13194.

582 64. Li J, Weinberger F, Saha M, Majzoub ME, Egan S. 2021. Cross-Host Protection of

583 Marine Bacteria Against Macroalgal Disease. Microb Ecol <https://doi.org/10.1007/s00248-021-01909-2>.

585 65. Burgunder-Delamare B, KleinJan H, Frioux C, Fremy E, Wagner M, Corre E, Le Salver

586 A, Leroux C, Leblanc C, Boyen C, Siegel A, Dittami SM. 2020. Metabolic Complementarity

587 Between a Brown Alga and Associated Cultivable Bacteria Provide Indications of Beneficial

588 Interactions. Front Mar Sci 7:85.

589 66. Mohr W, Lehn N, Ahmerkamp S, Marchant HK, Graf JS, Tschitschko B, Yilmaz P,

590 Littmann S, Gruber-Vodicka H, Leisch N, Weber M, Lott C, Schubert CJ, Milucka J, Kuypers

591 MMM. 2021. Terrestrial-type nitrogen-fixing symbiosis between seagrass and a marine

592 bacterium. Nature <https://doi.org/10.1038/s41586-021-04063-4>.

593 67. Noisette F, Hurd C. 2018. Abiotic and biotic interactions in the diffusive boundary layer

594 of kelp blades create a potential refuge from ocean acidification. Functional Ecology 32:1329–

595 1342.

596 68. Weigel BL, Pfister CA. 2020. Oxygen metabolism shapes microbial settlement on
597 photosynthetic kelp blades compared to artificial kelp substrates. *Environmental Microbiology*
598 Reports 1758-2229.12923.

599 69. Moulton O, Hacker S. 2011. Congeneric variation in surfgrasses and ocean conditions
600 influence macroinvertebrate community structure. *Mar Ecol Prog Ser* 433:53–63.

601 70. Howarth RW, Hobbie JE. 1982. THE REGULATION OF DECOMPOSITION AND
602 HETEROTROPHIC MICROBIAL ACTIVITY IN SALT MARSH SOILS: A REVIEW, p. 183–
603 207. *In* Estuarine Comparisons. Elsevier.

604 71. Martin BC, Middleton JA, Fraser MW, Marshall IPG, Scholz VV, Hausl B, Schmidt H.
605 2020. Cutting out the middle clam: lucinid endosymbiotic bacteria are also associated with
606 seagrass roots worldwide. *ISME J* 14:2901–2905.

607 72. Keller AH, Schleinitz KM, Starke R, Bertilsson S, Vogt C, Kleinstuber S. 2015.
608 Metagenome-Based Metabolic Reconstruction Reveals the Ecophysiological Function of
609 Epsilonproteobacteria in a Hydrocarbon-Contaminated Sulfidic Aquifer. *Front Microbiol* 6.

610 73. Helliwell KE. 2017. The roles of B vitamins in phytoplankton nutrition: new perspectives
611 and prospects. *New Phytol* 216:62–68.

612 74. Babbin AR, Tamasi T, Dumit D, Weber L, Rodríguez MVI, Schwartz SL, Armenteros M,
613 Wankel SD, Apprill A. 2021. Discovery and quantification of anaerobic nitrogen metabolisms
614 among oxygenated tropical Cuban stony corals. *ISME J* 15:1222–1235.

615 75. Fiore CL, Jarett JK, Olson ND, Lesser MP. 2010. Nitrogen fixation and nitrogen
616 transformations in marine symbioses. *Trends in Microbiology* 18:455–463.

617 76. Morris RL, Schmidt TM. 2013. Shallow breathing: bacterial life at low O₂. *Nature*
618 *Reviews Microbiology* 11:205–212.

619 77. Lilja EE, Johnson DR. 2019. Substrate cross-feeding affects the speed and trajectory of
620 molecular evolution within a synthetic microbial assemblage. *BMC Evol Biol* 19:129.

621 78. de Jesús Astacio LM, Prabhakara KH, Li Z, Mickalide H, Kuehn S. 2020. Closed
622 microbial communities self-organize to persistently cycle carbon. preprint, *Ecology*.

623 79. Goldford JE, Lu N, Bajić D, Estrela S, Tikhonov M, Sanchez-Gorostiaga A, Segrè D,
624 Mehta P, Sanchez A. 2018. Emergent simplicity in microbial community assembly. *Science*
625 361:469–474.

626 80. Hamersley MR, Sohm JA, Burns JA, Capone DG. 2015. Nitrogen fixation associated
627 with the decomposition of the giant kelp *Macrocystis pyrifera*. *Aquatic Botany* 125:57–63.

628 81. McGlathery K, Risgaard-Petersen N, Christensen P. 1998. Temporal and spatial variation
629 in nitrogen fixation activity in the eelgrass *Zostera marina* rhizosphere. *Mar Ecol Prog Ser*
630 168:245–258.

631 82. Garcias-Bonet N, Arrieta JM, Duarte CM, Marbà N. 2016. Nitrogen-fixing bacteria in
632 Mediterranean seagrass (*Posidonia oceanica*) roots. *Aquatic Botany* 131:57–60.

633 83. Steunou A-S, Jensen SI, Brecht E, Becroft ED, Bateson MM, Kilian O, Bhaya D, Ward
634 DM, Peters JW, Grossman AR, Kühl M. 2008. Regulation of nif gene expression and the
635 energetics of N₂ fixation over the diel cycle in a hot spring microbial mat. *ISME J* 2:364–378.

636 84. Cardini U, van Hoytema N, Bednarz VN, Al-Rshaidat MMD, Wild C. 2018. N₂ fixation
637 and primary productivity in a red sea *Halophila stipulacea* meadow exposed to seasonality: N₂
638 fixation in *Halophila stipulacea*. *Limnol Oceanogr* 63:786–798.

639 85. Agawin NSR, Gil Atorrasagasti MG, Frank Comas A, Fernández-Juárez V, López-
640 Alforja X, Hendriks IE. 2021. Response of the seagrass *POSIDONIA OCEANICA* and its associated
641 N₂ fixers to high business-as-usual climate change scenario in winter. *Limnol Oceanogr*

642 lno.11758.

643

644 Table 1. Summary of the features of 8 metagenomes. More information is in Table S1 and the
645 taxonomy based on single copy genes is in Table S2.

<i>Phyllospadix</i>		<i>Phyllospadix</i>		<i>Laminaria</i>	<i>Nereocystis</i>	<i>Zostera</i>	
	<i>scouleri</i>		<i>serrulatus</i>	<i>setchellii</i>	<i>luetkeana</i>		<i>marina</i>
Sediment	Rhizome	Blade	Rhizome	Blade	Inner bulb	Sediment	Rhizome
# quality reads (in millions)							
43.68	67.73	38.41	37.99	48.58	6.48	19.37	65.76
Bacteria							
63.7%	58.3%	63.6%	63.0%	63.9%	62.2%	33.6%	60.6%
Archaea							
34.2%	38.3%	33.1%	33.3%	32.7%	35.9%	62.1%	34.2%

646

647

648 Table 2. Metagenome assembled genomes across all samples and their representation across
 649 phyla. More detailed information on the MAGs can be found in Table S3.

<i>Phyllospadix</i>		<i>Phyllospadix</i>	<i>Laminaria</i>	<i>Nereocystis</i>	<i>Zostera</i>		
<i>scouleri</i>		<i>serrulatus</i>	<i>setchellii</i>	<i>luetkeana</i>	<i>marina</i>		
Sediment	Rhizome	Blade	Rhizome	Blade	Inner bulb	Sediment	Rhizome
High Quality MAGs							
3	1	7	6	9	1	2	5
Other MAGs							
2	2	8	7	7	0	5	7
Proteobacteria							
2	-	9	2	10	1	5	5
Bacteroidota							
3	2	5	4	4	-	-	1
Verrucomicrobia							
-	-	-	-	2	-	-	-
Campylobacterota							
-	-	-	-	-	-	2	1
Desulfobacterota							
-	-	-	2	-	-	-	3
Desulfuromonadota							
-	-	-	1	-	-	-	-
Acidobacteriota							
-	-	-	1	-	-	-	-
Spirochaetota							
-	-	-	1	-	-	-	-
No ID							
-	-	1	2	-	-	-	2
Crenarchaeota							
-	1	-	-	-	-	-	-

650

651

652

Figure Captions

653 **Figure 1.** Boxplot comparing the dissolved oxygen concentrations of water column (blue) and

654 the sediment-rhizome environment (red) of *P. scouleri* (pairwise t-test: $p < 0.001$) and *P.*

655 *serrulatus* (pairwise t-test: $p < 0.001$). Sampling dates are represented by different colors.

656

657 **Figure 2.** A phylogenomic tree of 6 concatenated bacterial single-copy core ribosomal genes

658 from 71 bacterial MAGS across 8 samples, showing the results from 33 high quality MAGs and

659 38 lower quality ones. One MAG, PSC_RHZ_Bin_00003, from the rhizome of *P. scouleri*, was

660 identified as an archaeal genome and was thus omitted from this tree. Gaps in class, family and

661 genus indicate the level to which taxonomic classification was resolved in each MAG. All blade

662 tissues have 'water column exposure', while rhizome and sediment samples do not.

663

664 **Figure 3.** Microbial Metabolisms in the MAGs reported in Fig. 2 and Table S3 across all hosts

665 and grouped as those that might benefit the host ("hosts benefit") and microbial metabolisms that

666 might utilize host provisioned metabolites ("microbes benefit"). Each tick along the x-axis

667 corresponds to a MAG. *N. luetkeana* blade MAGs are from Weigel et al. (in review). The

668 metabolisms for **DOC Uptake** that benefit microbes are shown as a heatmap of the count of the

669 number of genes that can metabolize *Compatible Solutes, Carboxylic Acids, Carbohydrate*

670 *Pentoses and General Carbohydrates*. Microbial metabolisms that benefit the host are

671 **Ammonification Hydrolases**, where the heatmap provides a count of the hydrolases acting on

672 C-N bonds other than peptide bonds, **Nitrogen Metabolisms** and **Vitamin** Synthesis, both

673 shown as the presence or absence of a gene in a pathway. The genes used in this are in Table S4.

674

675 **Figure 4.** A phylogenomic tree of *nifH* genes found on the rhizomes of *P. serrulatus* (PSE,
676 n = 3) and the rhizomes and surrounding sediment of *Z. marina* (ZMA, n = 2 and 5,
677 respectively). Some *nifH* genes group into Cluster I, including a sulfur oxidizing taxon on the
678 rhizome of *Z. marina*, and other taxa in *Campylobacterota*, including *Sulfurovum*. Cluster III
679 contains taxa associated with rhizomes including rhizomes including *Desulfobulbus*
680 *mediterraneus* on *P. serrulatus* and a Desulfobacterales associated with *Z. marina* rhizomes.
681

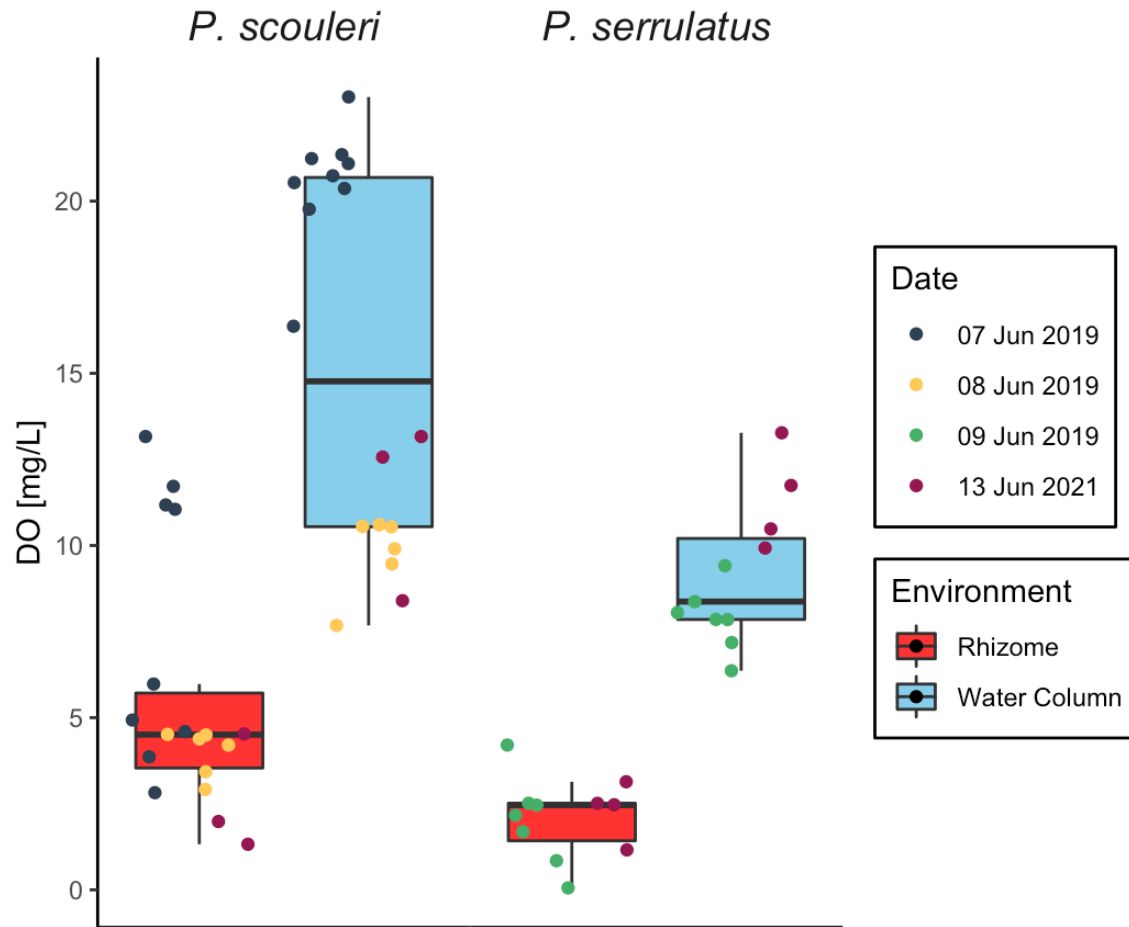
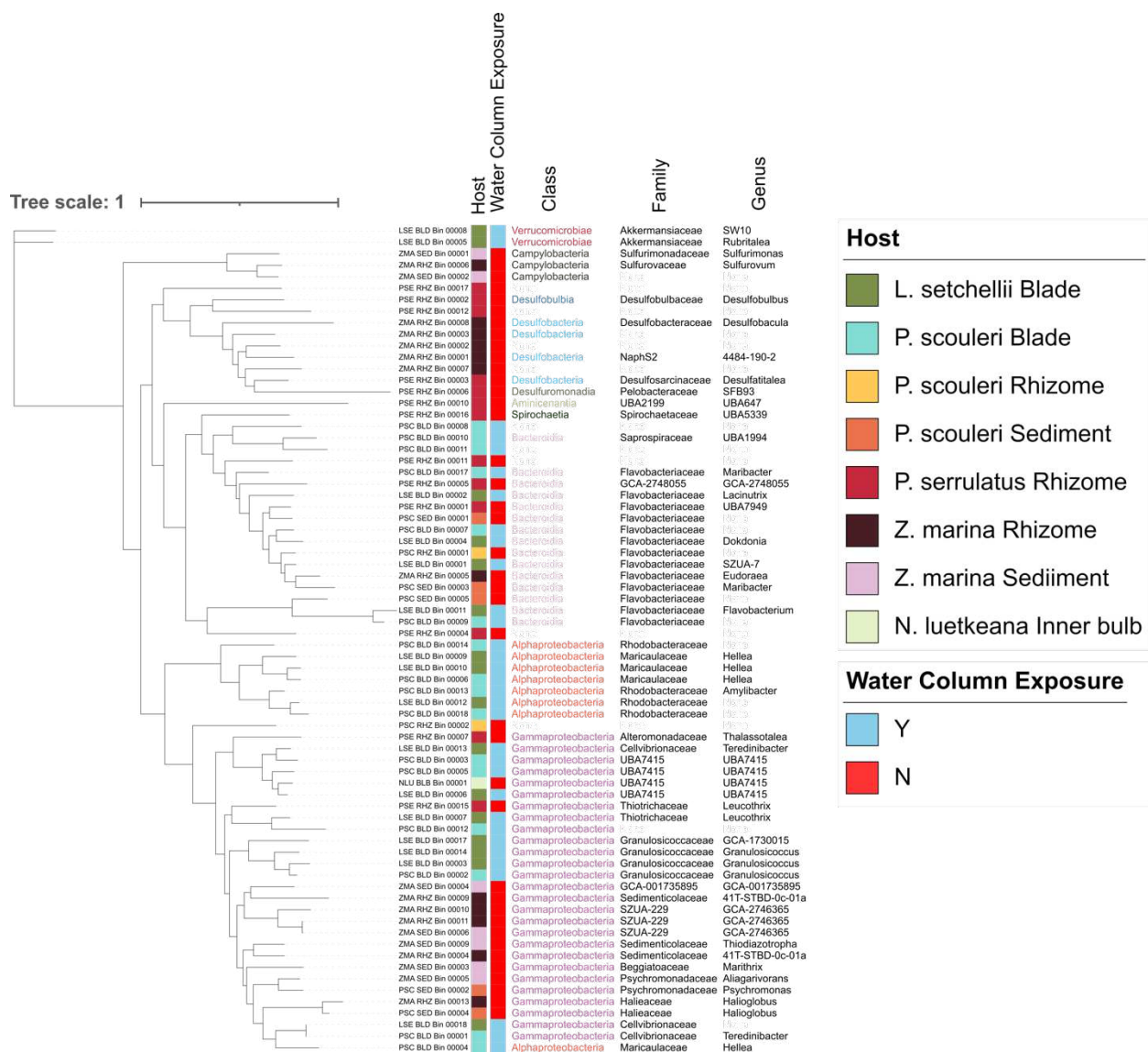


Figure 1

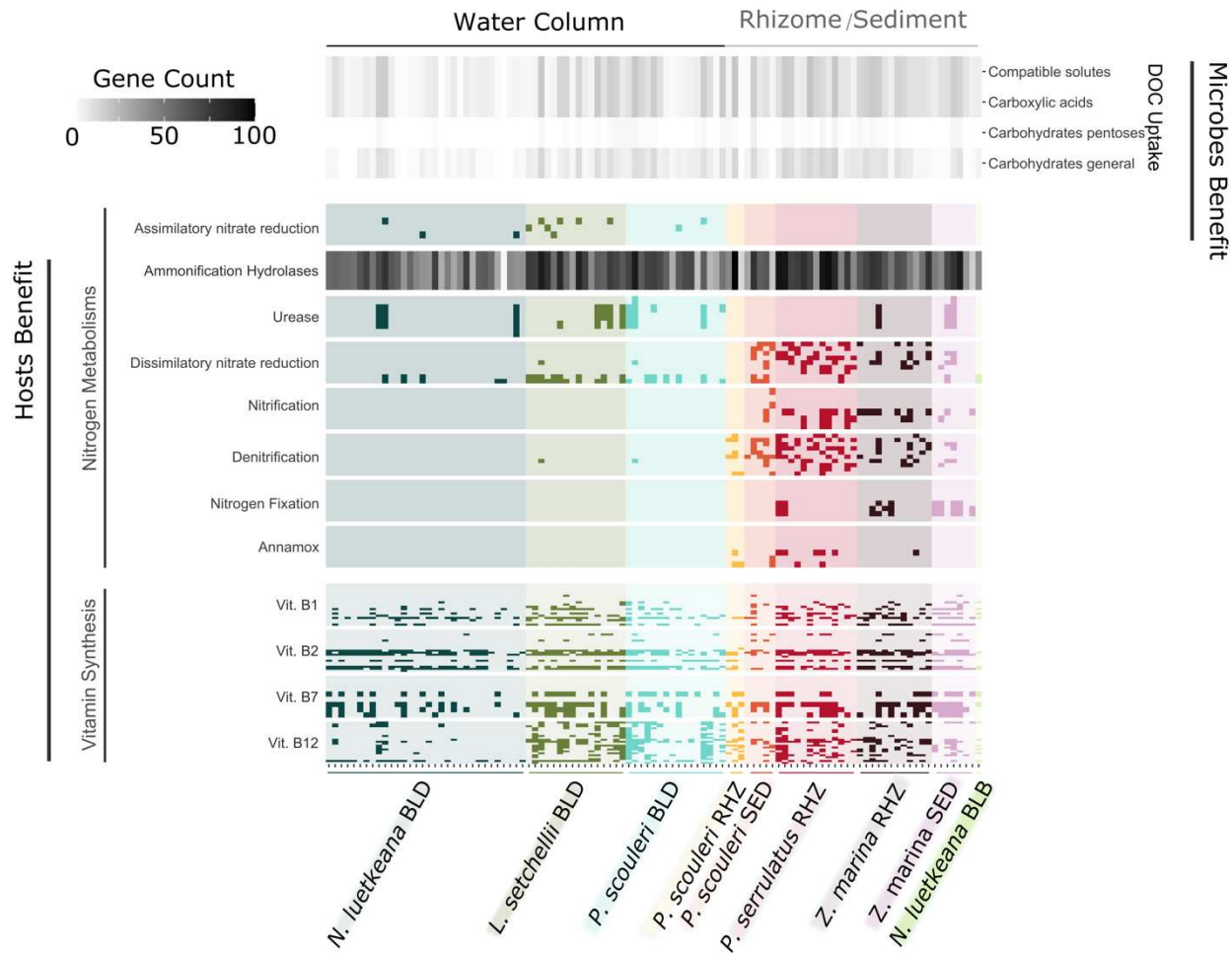
683



684

685

Figure 2



686

687

Figure 3

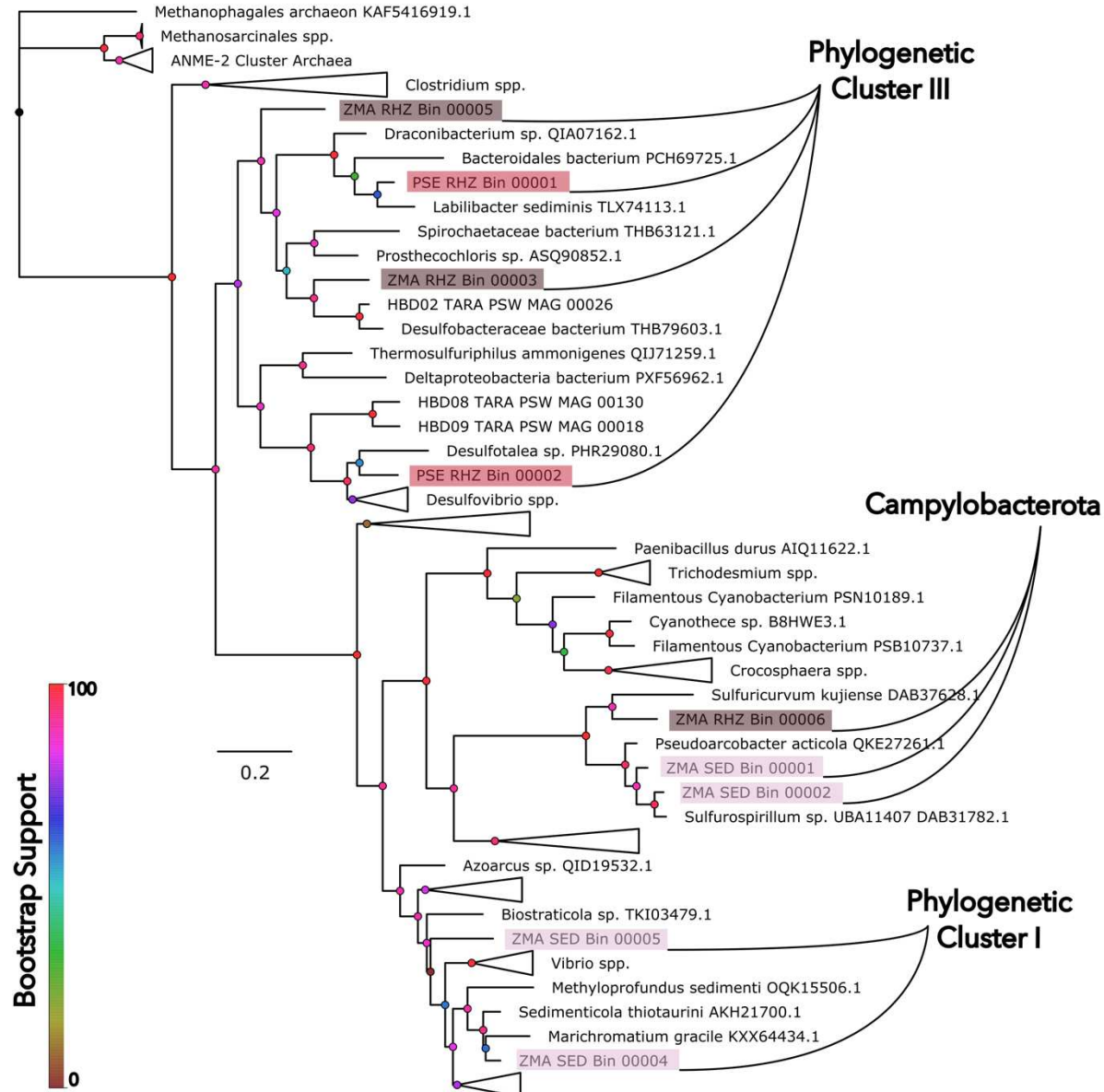


Figure 4

691

Supplementary Files

692 **Table S1.** A summary of eight metagenomes from five macrophyte taxa.

693 **Table S2.** A summary of taxonomy of MAGs

694 **Table S3.** The features of 72 metagenome assembled genomes (MAGs).

695 **Table S4.** Genes used to generate Fig. 3

696 **Table S5.** The features of *nifH* genes found in MAGs.

697 **Table S6.** *nifH* reference amino acid sequences

698

699 **Appendix 1.** Additional methods to quantify carbon and nitrogen stable isotopes in *P. scouleri*

700 **Figure S1.** Stable isotope analysis of delC13 and delN15 at blade tip, meristem, rhizome of *P.*

701 *scouleri*. From blade tip to rhizome, water flow and thus elemental mixing reduces due to

702 attenuation and boundary layer effects of surfgrass canopy. Assuming elemental uptake occurs

703 from the same pools of C and N, the lower the extent of mixing, the heavier the isotopic

704 signature should be at that point of the plant. This is observed with delC13 which gets heavier

705 from the tip to the blade. This is observed with delN15 till the meristem after which it lightens.

706 This is probably occurring as nitrogen is taken up from a different pool of nitrogen from that

707 around the blade/meristem. This different pool is probably made available through n-fixation